

1 DOI: <https://doi.org/10.36253/ijam-3676>

2

3 **Monitoring Drought Impacts through Spatiotemporal Analysis of Climatic and**
4 **Vegetative Indices in the Drâa River Watershed, Morocco**

5 Kaouthar Majdouli^{1*}, Ahmed Algouti¹, Najat Bhiry², John Molson³, Abdellah Algouti¹, Khadija
6 Lamrani¹, and Imane El Kihal¹.

7 ¹ Laboratory of Geosciences, Geotourism, Natural Hazards and Remote Sensing, Faculty of Sciences Semlalia,
8 Cadi Ayyad University, Boulevard Prince My Abdellah, B.P. 2390, 40000 Marrakech, Morocco

9 ² Department of Geography, Université Laval, Pavillon Abitibi-Price, 2405, rue de la Terrasse, Quebec G1V 0A6,
10 Canada

11 ³ Department of Geology and Geological Engineering, Université Laval, Pavillon Adrien Pouliot 1065, avenue
12 de la Médecine, Local 4309, Québec G1V 0A6, Canada

13 Emails : k.majdouli.ced@uca.ac.ma (Corresponding author*), algouti@uca.ac.ma, Najat.Bhiry@rec.ulaval.ca,
14 john.molson@ggl.ulaval.ca, abalgouti@uca.ac.ma, k.lamrani.ced@uca.ac.ma, i.elkihal.ced@uca.ac.ma

15 Orcid : 0009-0000-1118-4819*, 0000-0002-2344-0821, 0000-0002-6609-0235, 0000-0002-6581-8044, 0000-
16 0001-7501-5221, 0009-0000-8350-2935, 0009-0004-0737-120

17 **Abstract**

18 The Drâa River watershed, characterized by a semi-arid climate, is particularly vulnerable to
19 the risk of desertification, a threat exacerbated by the effects of global warming. This study is
20 based on an analysis of climatic and hydrological variations in the Drâa basin, using satellite
21 and terrestrial data. Climatic indices including SPI and PDSI, and vegetation indices VCI, TCI,
22 VHI and NDVI, were calculated to assess the impact of climatic conditions on water resources
23 and vegetation cover. In addition, the water reflectance index (NDWI) was used to analyze
24 variations in water level of the El Mansour Eddahbi reservoir. The remote sensing results were
25 compared with records from local hydrological stations to ensure consistent and thorough
26 interpretation. The analyses show that the Drâa watershed is currently experiencing the longest
27 drought in its recorded history, although its intensity is lower than that observed between 1981
28 and 1984. Over a 23-year period (2000-2023), only 9 years were relatively wet, compared to
29 14 years of drought, according to the SPI index. These climatic conditions have put considerable
30 pressure on water resources and vegetation cover, as evidenced by variations in vegetation
31 indices and climatic parameters. The reduction in the surface area and perimeter of the El
32 Mansour Eddahbi reservoir, observed by remote sensing, was corroborated by the decrease in

33 water volume measured in situ. Prolonged droughts in this region therefore pose a significant
34 threat to water and environmental resources.

35 **Keywords:** Drought, Remote sensing, Climatic indices, Vegetative indices, Climate change

36 **Highlights**

37 • The impacts of drought were assessed in the Drâa basin using satellite indices.
38 • Significant vegetative stress was detected during the main drought episodes.
39 • Strong correlations confirm the influence of climatic factors on vegetation.
40 • Validation tests, based on ground data, confirmed the reliability of the results.

41 **Introduction**

42 Drought, a recurring natural phenomenon with dramatic consequences, is one of the most
43 complex challenges facing arid and semi-arid regions such as Morocco. Although drought is
44 not a new concept in Morocco (the country has always experienced alternating dry and wet
45 periods), in recent years, the frequency of periods vulnerable to drought risk has become
46 increasingly important and alarming (Stour & Agoumi, 2008; Hadria et al. 2019; Lahbous,
47 2023; Gumus et al., 2024; Bijaber et al., 2024). With an economy largely based on agriculture,
48 Morocco therefore faces major challenges related to increasing aridity, especially in its arid and
49 semi-arid regions (Hadri et al., 2022; Lebdi & Maki, 2023).

50 At the national level, the impacts of drought are not limited to the environment. In economic
51 terms, for example, the effects are significant. (Lahbous, 2023) shows that successive droughts
52 have caused a significant decline in agricultural value added, which has significantly reduced
53 the national gross domestic product (GDP). This situation exacerbates the vulnerability of the
54 rural population and threatens the country's food security. In 2017, the World Bank published a
55 report on environmental costs in Morocco (Dahan, 2017), estimating that environmental
56 degradation accounts for a loss of about 3.5% of national GDP. Among these costs, the
57 degradation of water resources stands out, accounting for around 1.6% of GDP, surpassing air
58 pollution, which in turn accounts for 1.05% of GDP. In addition, degraded soils, affected by
59 erosion and land conversion into desertified areas, also contribute significantly to environment-
60 related economic losses (Dahan, 2017).

61 In this context, the Drâa River watershed, a semi-arid region in southern Morocco, stands out
62 for its increased vulnerability to drought. The Drâa watershed is particularly vulnerable due to

63 its dependence on groundwater to meet the needs of the local population (Ouysse et al., 2010).
64 However, this vital resource is seriously threatened by persistent meteorological drought,
65 exacerbated by extreme adverse weather conditions. Rainfall deficits, coupled with rising
66 temperatures and a wide temperature range, are significantly reducing wetlands, with direct
67 impacts on vegetation cover, surface water and groundwater (Saouabe et al., 2022; Sadiki &
68 Hanchane, 2024). Adverse climatic conditions, combined with increasing demographic and
69 industrial pressures, have placed the Drâa basin in a critical and alarming situation. In response
70 to these challenges, it has become imperative to implement rigorous management strategies to
71 preserve the region's water resources.

72 In this context, several studies have been conducted to map the areas most affected by the
73 adverse effects of meteorological drought (Auclair, 1987; Agoussine et al., 2003, 2004; Schulz
74 et al., 2004, 2008; Weber, 2004; Aït Hamza et al., 2010; Ouysse et al., 2010; Bentaleb, 2011,
75 2015; Baki et al., 2017; Mehdaoui et al., 2018; El Qorehi et al., 2023). However, drought
76 management in this region, particularly in terms of forecasting and assessing its impact on water
77 resources, remains a major challenge. When it comes to studying and managing climate risks,
78 the availability of in situ climate and hydrological data, as well as the methods used to collect
79 this information, continue to be key obstacles (Wang et al., 2015; Aksu et al., 2022b). New
80 space technologies and remote sensing tools provide a variety of capabilities for monitoring
81 climatic phenomena over large areas and long periods of time (Ji & Peters, 2003; Hao & Singh,
82 2015; Wang et al., 2015; Li et al., 2016; Bijaber & Rochdi 2017; Eyoh et al., 2019; Bashit et
83 al., 2022; Houmma et al., 2023; Serboui et al., 2023). The use of satellite sensors has replaced
84 the traditional method based on calculating climate indices from terrestrial data measured and
85 recorded by a limited network of meteorological and hydroclimatic stations. These stations are
86 often inadequate and unrepresentative, especially in desert regions, which make up a significant
87 portion of the catchment area under study. Moreover, many climate indices require data series
88 of at least 30 years to provide convincing results. To illustrate, hydroclimatic indices such as
89 the Standardized Precipitation Index (SPI), the Standardized Precipitation-Evapotranspiration
90 Index (SPEI) (McKee et al. 1993), and the Palmer Drought Severity Index (PDSI) (Palmer,
91 1965; Li et al., 2016; Zkhiri et al., 2018; Kim et al., 2021) are often used to assess hydroclimatic
92 drought over large spatiotemporal areas. In this context, several studies have been conducted to
93 use satellite data in the study of drought in Morocco. The analysis of the Palmer Drought Index
94 (PDSI) by de Waroux in 2013 revealed a clear trend of increasing drought in the Aoulouz argan
95 grove region over the last few decades, mainly due to the increase in mean annual temperatures,

96 thus higher evapotranspiration and less recharge. In fact, the increase in temperature appears to
97 be the main factor affecting the health of argan trees, limiting their natural regeneration and
98 accelerating the degradation of the local ecosystem. According to [Elair et al. \(2023\)](#), the use of
99 SPI, VCI, TCI, and VHI indices showed that the Marrakech-Safi region experienced significant
100 variations in drought frequency between 1984 and 2022, with periods characterized by
101 moderate to severe drought events. Several critical droughts were identified from 1981 to 2017,
102 interspersed with periods of rainfall. However, studies indicate an increasing trend in the
103 frequency, duration and intensity of droughts in recent decades, highlighting the challenges of
104 water resource management and agriculture in the region ([Choukrani et al., 2018](#)). Combined
105 analyses of remote sensing indices such as SPI, SPEI, STI, TCI and GRACE-DSI have revealed
106 a significant worsening of drought episodes in the Bouregreg catchment located in the north-
107 western part of Morocco. This intensification is not the result of a significant decrease in
108 precipitation, which has remained stable overall, but rather of a growing water imbalance,
109 fueled by a significant increase in temperature. The increase in evapotranspiration catalyzed by
110 global warming has thus exacerbated the agricultural and hydrological forms of drought in the
111 region ([Ait Dhmane et al, 2024](#)).

112 The Drâa watershed is no exception to the recent national trend of increasing drought. However,
113 its vast surface area and the diversity of its topographic and climatic conditions make
114 monitoring this phenomenon particularly complex. The objective of this study is to assess the
115 risk of drought in the basin using several indices derived from satellite data for the period
116 between 1960 and 2023. More specifically, it aims to analyze the spatial and temporal
117 variability of drought using satellite indices based on reflectance and brightness temperature,
118 to evaluate their performance in detecting drought events and their frequency, and to identify
119 the most vulnerable areas of the Drâa watershed. These indices are then compared with field
120 data provided by the Drâa-Oued Noun Water Basin Agency, as well as with trend analyses of
121 raw climatic parameters such as precipitation and temperature.

122 **Materials and methods**

123 **Study area**

124 The Drâa River watershed is located in the southern part of Morocco and covers an area of
125 approximately 93,729 km². It is bounded to the north by the foothills of the High Atlas, from
126 Jbel Toubkal to Jbel M'Goun, and to the south by the Saharan basin and the border with Algeria.
127 It is bordered to the east by the Todgha and Rhis valleys and to the west by the Guelmim and

128 Souss Massa basins (Figure 1). The Drâa is a region where geography, geology and the
 129 availability of water resources are closely linked. Its climate, which is semi-arid in the north
 130 and becomes Saharan south of M'Hamid El Ghizlane, is mainly influenced by its geographical
 131 position between the High Atlas and the Anti-Atlas, as well as its proximity to the Atlantic
 132 Ocean (DRPE, 2008; Schulz et al., 2004). The region suffers from pronounced aridity,
 133 especially in the Anti-Atlas, although cool winds from the Atlantic bring some moderation to
 134 the climate. However, the high frequency of anticyclones contributes to a severe lack of
 135 precipitation (ABHDON, 2009). From a hydrological point of view, the Drâa basin includes the
 136 longest river (Drâa River) in Morocco, with a length of 1100 km. It rises at the confluence of
 137 the Dadès and Ouarzazate rivers, at the El Mansour Eddahbi dam, and follows a winding course
 138 before emptying into the Atlantic Ocean. This great length crosses a variety of geographical and
 139 topographical contexts, giving rise to a division into the Upper, Middle and Lower Drâa, each
 140 with distinct geographical and hydrological characteristics (Figure 1) (ABHDON, 2013).

141

142

143

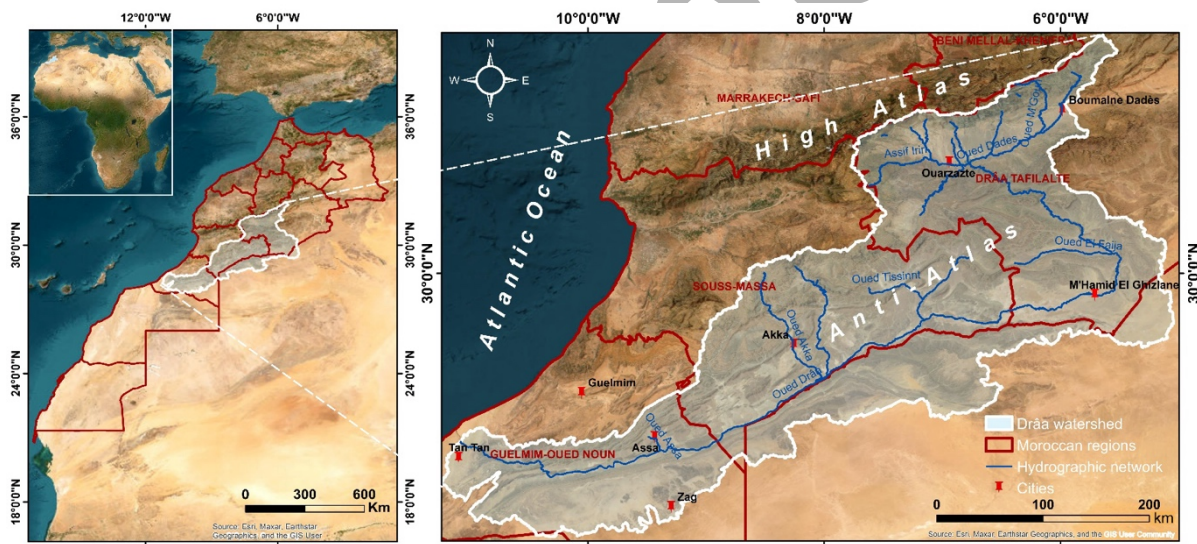
144

145

146

147

148



149

150

Figure 1. Location map of the study area showing the Drâa River watershed situated in southern Morocco.

151

Data sources

152

Remote sensing data

153

a) NOAA and VIIRS sensor images

154 The National Oceanic and Atmospheric Administration (NOAA) is a platform equipped with a network
155 of satellites, ocean buoys, meteorological stations and other instruments designed to collect variable
156 precision, real-time information on climatic and oceanic conditions worldwide. These data are publicly
157 accessible via a number of digital platforms. In order to characterize the meteorological aridity of our
158 vast study area over a period of about forty years, we used data presented by NESDIS STAR (National
159 Environmental Satellite, Data, and Information Service - Center for Satellite Applications and
160 Research), accessible through the link .

161 A detailed analysis of environmental conditions and climate trends using indices based on
162 precipitation, temperature and evapotranspiration potential was made possible by using the
163 TerraClimate database. This high-resolution data source (approximately 4 km resolution) provides a
164 monthly overview of a number of hydrological and climatic variables essential for characterizing
165 drought in a given region. The data are available from 1958 to the present and can be accessed free of
166 charge at <http://www.climatologylab.org/terraclimate.html>.

167 **b) Google Earth Engine data**

168 In order to document the spatiotemporal variation of the normalized vegetation index, we used the
169 Google Earth Engine platform (<https://code.earthengine.google.com/>), which provides a large
170 collection of historical and current satellite data from different sensors such as Landsat, MODIS and
171 Sentinel. For this purpose, we used Java scripts to visualize NDVI maps of the Drâa watershed based
172 on data extracted from Landsat 5 satellite sensors for the years 1984, 1989, 1994, and 1999, as well as
173 from the MOD13Q1 satellite sensor for the years 2000-2023. The resulting maps are then stored,
174 processed, and used to monitor drought trends over time.

175 **Data from land based hydrological stations: Precipitation and volume variations of the El
176 Mansour Eddahbi Dam**

177 Gathering stations provide accurate and localized rainfall measurements that are essential for the
178 calibration and verification of satellite data. These stations were established and are currently managed
179 by the Drâa Oued Noun Water Basin Agency. Based on a network of 27 rain gauge stations distributed
180 upstream and downstream in the Drâa basin, we were able to establish interpolations based on real
181 data, allowing us to assess the validity and accuracy of the results obtained by remote sensing
182 platforms.

183 Because we work with satellite data, it is essential to perform pre-processing on downloaded images
184 to ensure data reliability and quality. For information presented in image form, we have applied the

185 necessary atmospheric and radiometric corrections. These are aimed at adjusting pixel values to correct
186 for variations in sensor sensitivity and aligning images to correct for geometric distortions. As for the
187 data corresponding to point measurements of climatic parameters at specific stations, usually acquired
188 in CSV (comma-separated values) format, we prepared the database by selecting the time intervals and
189 calculating the monthly and annual sums and averages for each climatic parameter to be used in the
190 calculation of the indices. These preliminary steps are crucial before proceeding with spline
191 interpolation with barriers to obtain the final map. In general, the approach used in this study aims to
192 monitor drought trends over a 50-year period, focusing on the current situation (Figure 2). This
193 monitoring was done using satellite climate indices from NOAA, TerraClimate and Google Earth
194 Engine. A large watershed like the Drâa, with inaccessible desert areas, poses enormous problems in
195 terms of data availability. In this study, new space technology has proven very useful, with online
196 information used to produce maps suitable for management and decision-making in these areas. The
197 resulting cartographic maps were validated using real data collected along the Drâa River, based on a
198 correlation between the products of the different data sources.

199 Severe weather conditions have a significant impact on the size of water reservoirs. In this regard, as
200 a third validation, we used the large El Mansour Eddahbi reservoir in the Drâa watershed as a reference.
201 Using the Normalized Difference Water Index (NDWI) and volume measurements carried out by the
202 Drâa Oued Noun Water Basin Agency, we carried out a detailed study of the temporal variation of its
203 surface area and perimeter in order to identify dry and wet years for this reservoir, which receives most
204 of its annual rainfall from the Tidili-Iriri and Dadès-M'Goun tributaries.

205 **Drought indices**

206 **a) Reflectance-Based Indices**

207 **NDVI (Normalized Difference Vegetation Index)**

208 Proposed by (Rouse et al., 1973) as an index of vegetation health and density, NDVI is currently
209 considered the most widely used indicator for monitoring terrestrial vegetation over large areas. This
210 index is defined by the following formula:

$$211 \quad NDVI = \frac{NIR - RED}{NIR + RED}$$

212 where NIR and RED are reflectances in the near infrared and red bands, respectively. NDVI varies
213 from -1 to +1, with positive values close to 1 indicating dense, healthy vegetation, and low negative
214 values indicating a lack of vegetation or non-vegetated surfaces, which can be water or bare soil.

215 **VCI (Vegetation Condition Index)**

216 The VCI is a vegetative stress index expressed as a function of maximum, current and minimum NDVI
217 values over a period of time (Liu & Kogan 2002). It differs from NDVI in its ability to analyse
218 vegetation conditions for heterogeneous areas (Kogan, 1990), which is due to its ability to separate the
219 short-term climatic signal from the long-term ecological signal (Kogan & Sullivan, 1993). VCI values
220 generally vary between 0 and 100, with a zero value corresponding to extremely poor vegetation
221 conditions and maximum values close to 100 indicating optimal vegetation conditions, and can be
222 defined as:

223
$$VCI = \frac{NDVI - NDVI \min}{(NDVI \max - NDVI \min)} \times 100$$

224 **NDWI (Normalized Difference Water Index)**

225 The NDWI introduced by (McFeeters, 1996) is a reflectance-based index commonly used to identify
226 and monitor the presence of water on the Earth's surface. The NDWI uses reflected radiation in the
227 near infrared and visible green light to enhance the presence of water features while eliminating the
228 presence of soil and terrestrial vegetation (McFeeters, 1996). The NDWI formula is generally defined
229 as follows:

230
$$NDWI = \frac{(Green - NIR)}{(Green + NIR)}$$

231 **b) Brightness Temperature-Based Indices**

232 **TCI (Temperature Condition Index)**

233 This thermal index is essentially based on the Earth's surface temperature. It was developed at NOAA
234 in 1995 (Kogan, 1997), and is calculated using images from NOAA's AVHRR sensor. This index is
235 very useful for characterizing thermal stress over long periods of time and over large areas (Kogan,
236 1997). Combined with other vegetation indices such as VCI, it provides a more comprehensive
237 assessment of the vegetation condition of a given area. It is calculated as follows (Layelmam, 2015):

238

239
$$TCI = \frac{LST \ max - LST (i)}{LST \ max - LST \ min}$$

240 where LST_{max} is the maximum surface temperature of the period studied, LST_{min} is the minimum
241 surface temperature of the period studied and $LST(i)$ is the surface temperature of the month
242 concerned.

243 **c) Combined Reflectance and Brightness Temperature-Based Indices**

244 **VHI (Vegetation Health Index)**

245 Because it combines a thermal factor and plant reflectance, the VHI is the most appropriate indicator
246 for vegetation. This index was developed by (Kogan, 1995), and is very effective in terms of studying
247 and managing agricultural drought by assessing vegetation health. It works by combining the
248 Vegetation Condition Index (VCI) and the Temperature Condition Index (TCI), while relying on their
249 negative correlation, to detect, monitor and provide early warning of the frequency and intensity of
250 agricultural drought (Justice et al. 1998; Seiler et al. 1998). It is expressed by the following equation:

251
$$VHI = \alpha \cdot VCI + \beta \cdot TCI$$

252 where α and β are coefficients assigned to each of these combination factors and refer to the negative
253 correlation between the thermal index and the plant index. These coefficients are equal to 0.5,
254 according to (Wilhite et al., 2000).

255 **d) Rainfall variation-based indices**

256 **SPI (Standardized Precipitation Index)**

257 The SPI index (McKee et al., 1993, 1995) is a powerful yet easy to calculate tool that requires
258 only precipitation data to quantify precipitation deficits or surpluses. It measures variations in
259 precipitation relative to historical averages over a specified period, whether deficit or surplus,
260 over periods ranging from 3 months to 2 years. Its optimal calculation requires monthly
261 measurements over 20 to 30 years, ideally 50 to 60 years, although missing data can affect the
262 reliability of the results (WMO, 2012). The SPI index can be expressed as:

263
$$SPI = \frac{P - P_m}{\sigma P}$$

264 where P is the total precipitation for a given period (mm), P_m is the historical mean precipitation
265 for the period (mm), and σP is the historical standard deviation of precipitation for the period
266 (mm).

268 **PDSI (Palmer Drought Severity Index)**

269 The PDSI is a meteorological drought index developed by Palmer (Briffa et al., 1994; Scian &
 270 Donnari, 1997; Cook et al., 1999). Its ultimate goal is to provide standardized measurements of
 271 moisture conditions so that comparisons can be made using this index between different
 272 locations and between different months. To achieve this, the PDSI relies on data on
 273 precipitation, current and past temperatures, and available soil moisture (Mika et al., 2004),
 274 However, it does not directly consider surface hydrological resources (groundwater, rivers,
 275 reservoirs), that can influence drought conditions (Layelmam, 2015). The PDSI index is
 276 calculated using:

277
$$PDSI = X(i) = \frac{0.897 X(i-1) + Z(i)}{3}$$

278 where X (i-1) is the PDSI of the previous period, and Z(i) is the moisture anomaly index
 279 which is calculated by the following formula:

280
$$Z(i) = K(P - P_c)$$

281 where K is a weighting factor (see Alley 1984), P is the current precipitation (mm), and P_c is
 282 the CAFEC precipitation (mm; *Climatically Appropriate for Existing Conditions*), representing
 283 the amount of rainfall needed to maintain a balanced water supply (i.e., neither drought nor
 284 excessive humidity) under normal climatic conditions. It is expressed as: CAFEC = Potential
 285 Evapotranspiration (PE) + Recharge + Runoff – Soil Moisture Loss/Gain.

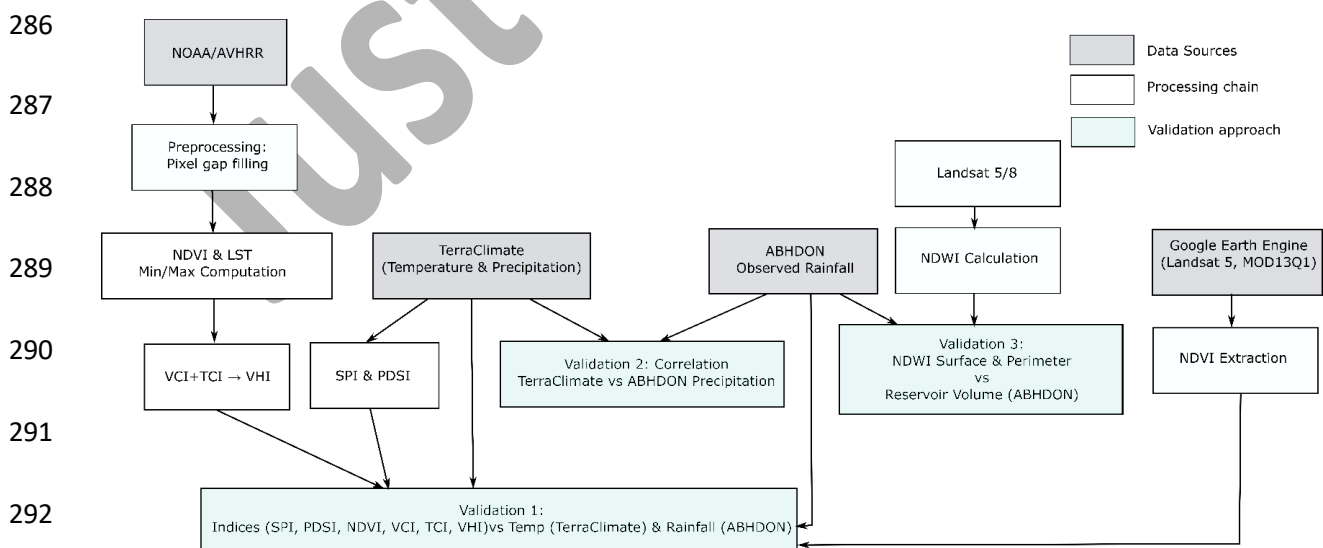
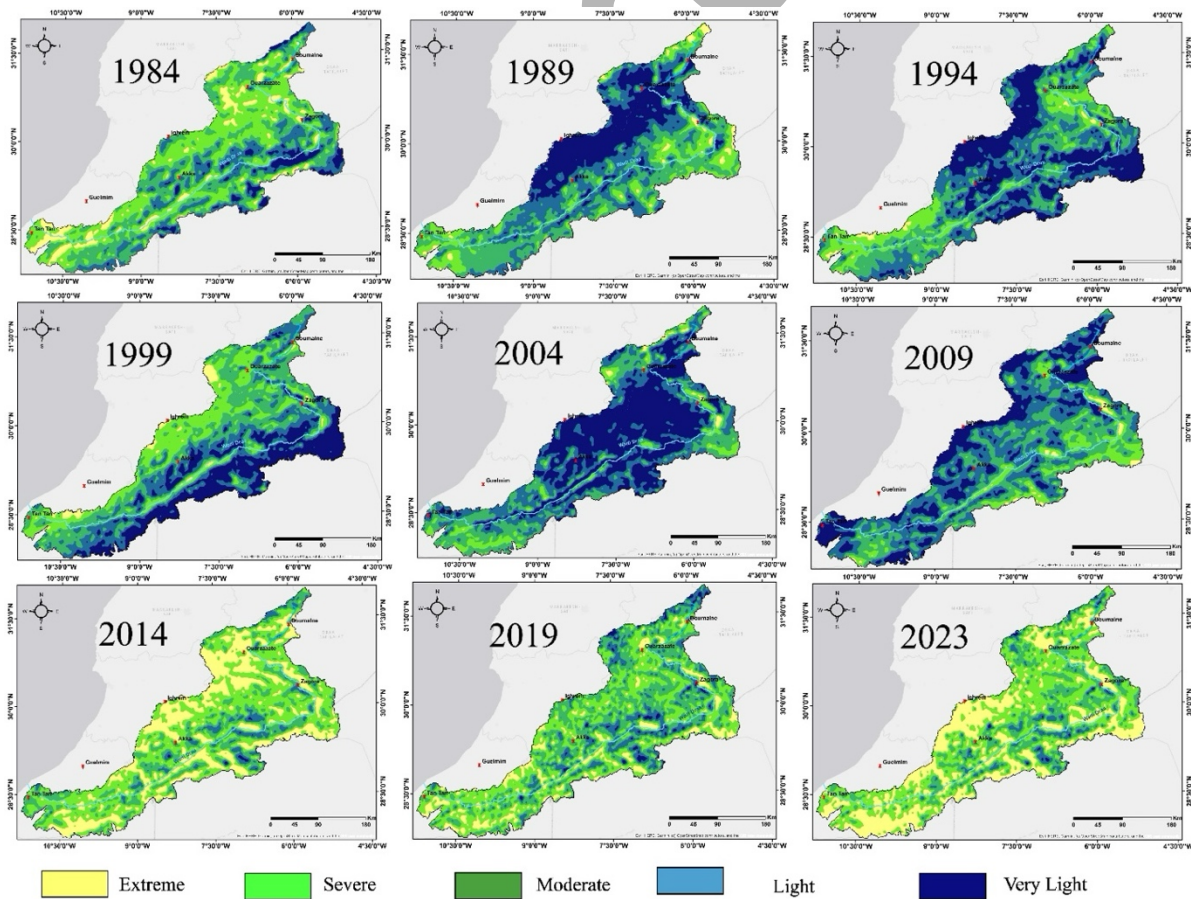


Figure 2. Workflow diagram illustrating the main steps of the adopted work methodology.

295 **Results**296 **Reflectance-Based Indices**297 **VCI**

298 The map of spatiotemporal variation of the Vegetation Condition Index (VCI) (Figure 3) shows
 299 an increasing trend towards drought between 1984 and 2023. During the period from 1989 to
 300 2009, conditions appear relatively normal, with slight fluctuations observed between 1989 and
 301 2009, and spatially between the High Atlas and Anti-Atlas regions. These fluctuations can be
 302 attributed to topographic variations, which have a direct influence on the amount of
 303 precipitation and the diurnal temperature variations. In fact, the varied topography of the
 304 mountainous areas of the High Atlas and Anti-Atlas results in distinct microclimates. Higher
 305 altitudes generally receive more precipitation, while lower areas can be more arid. Since 2009,
 306 a significant increase in drought has been observed, leading to a progressive deterioration of
 307 vegetation conditions and an increase in periods of water stress. This deterioration could be
 308 linked to climate change, which is strongly affecting precipitation patterns and temperatures.

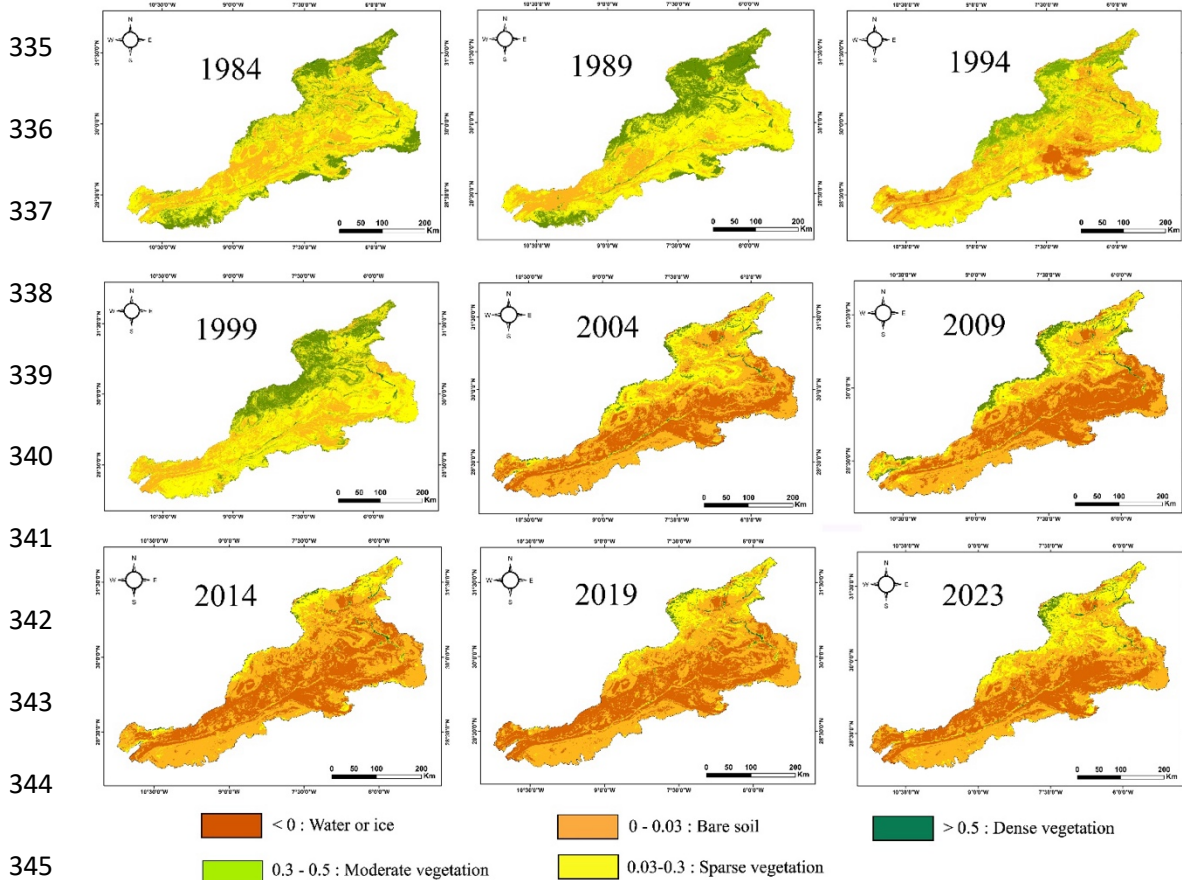


321 **Figure 3.** Spatiotemporal variation map of the Vegetation Condition Index (VCI).

322 **NDVI**

323 Analysis of the normalized vegetation index (NDVI) in Figure 4 clearly indicates a significant
 324 shift in the climatic conditions of the Drâa watershed since the 2000s. Even land in the Atlas
 325 regions shows progressively lower NDVI values, specially from 2004 to 2023. Bare soil and
 326 Saharan zones occupy about three quarters of the watershed surface area, which is explained
 327 by regional climatic conditions. These changes indicate a gradual degradation of vegetation
 328 cover, highlighting water stress and a decline in biological productivity. Analysis of the NDVI
 329 data during this period shows the severe impact of the climatic conditions on the ecosystem of
 330 the Drâa watershed. Green zones with high NDVI values continue to show resilience,
 331 especially in the foothills of the high mountains, largely benefiting from the effect of
 332 snowmelt. These areas of dense vegetation also extend along the Drâa River, from the High
 333 Dadès in the east and Tidili-Iriri in the west, to Mhamid El Ghizlane in the south (Figure 1).

334

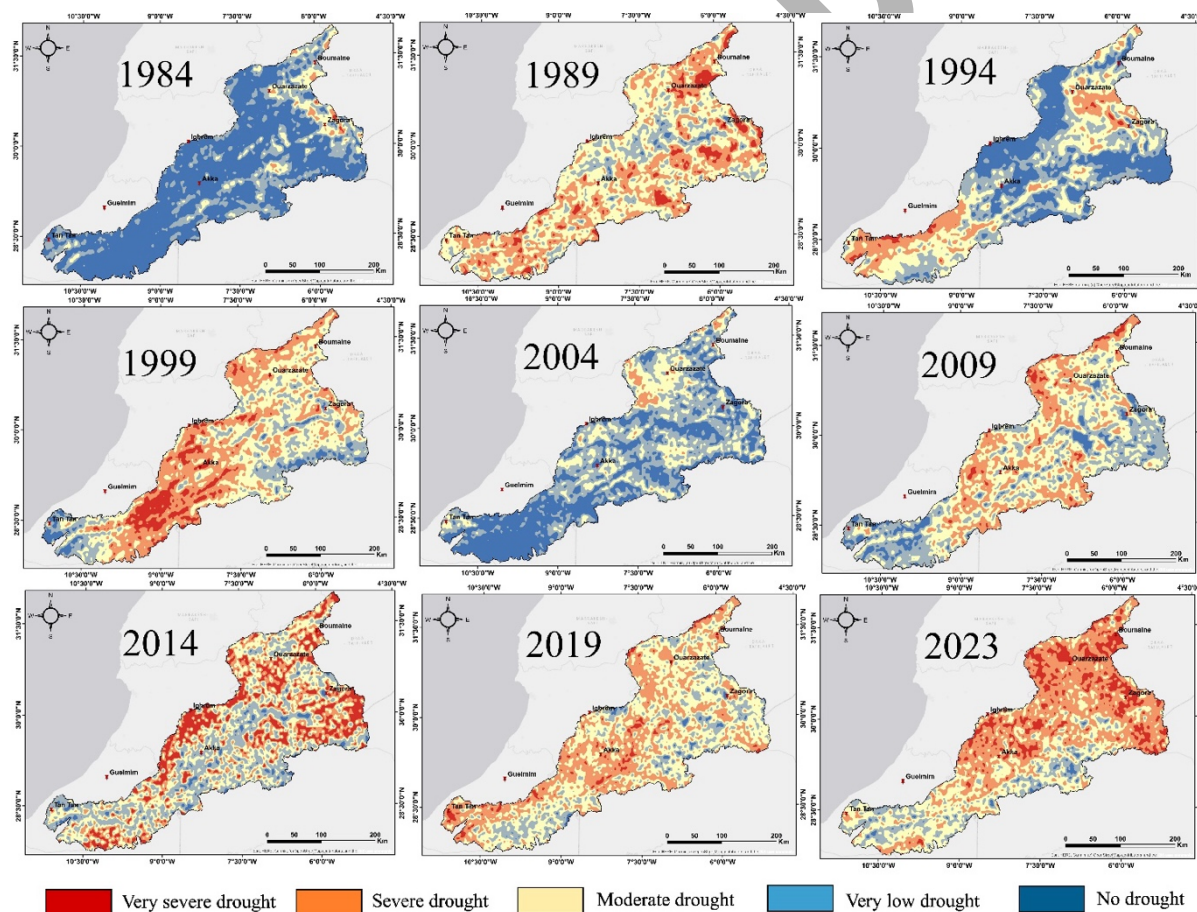


346 **Figure 4.** Normalized Difference Vegetation Index (NDVI) map illustrating spatial variations
 347 in vegetation cover across the study area.

348 **Brightness Temperature-Based Indices**349 **TCI**

350 As shown in Figure 5, the temporal variation of the temperature condition index (TCI) shows
 351 some cyclicity. Any year with extremely high temperatures could indicate a period of drought,
 352 followed four years later by a year with lower temperatures, indicating wet conditions.

353 This index examines the effect of temperature on vegetation, showing that even the lowest
 354 temperatures can have a negative effect on plant cover. Therefore, it is important to use this
 355 index alongside the Vegetation Condition Index (VCI) rather than in isolation. The combination
 356 of these two indices results in the Vegetation Health Index (VHI). Basically, years with
 357 favorable vegetation conditions are confirmed by the VHI, enhancing the reliability of the
 358 conclusions drawn from their analysis.

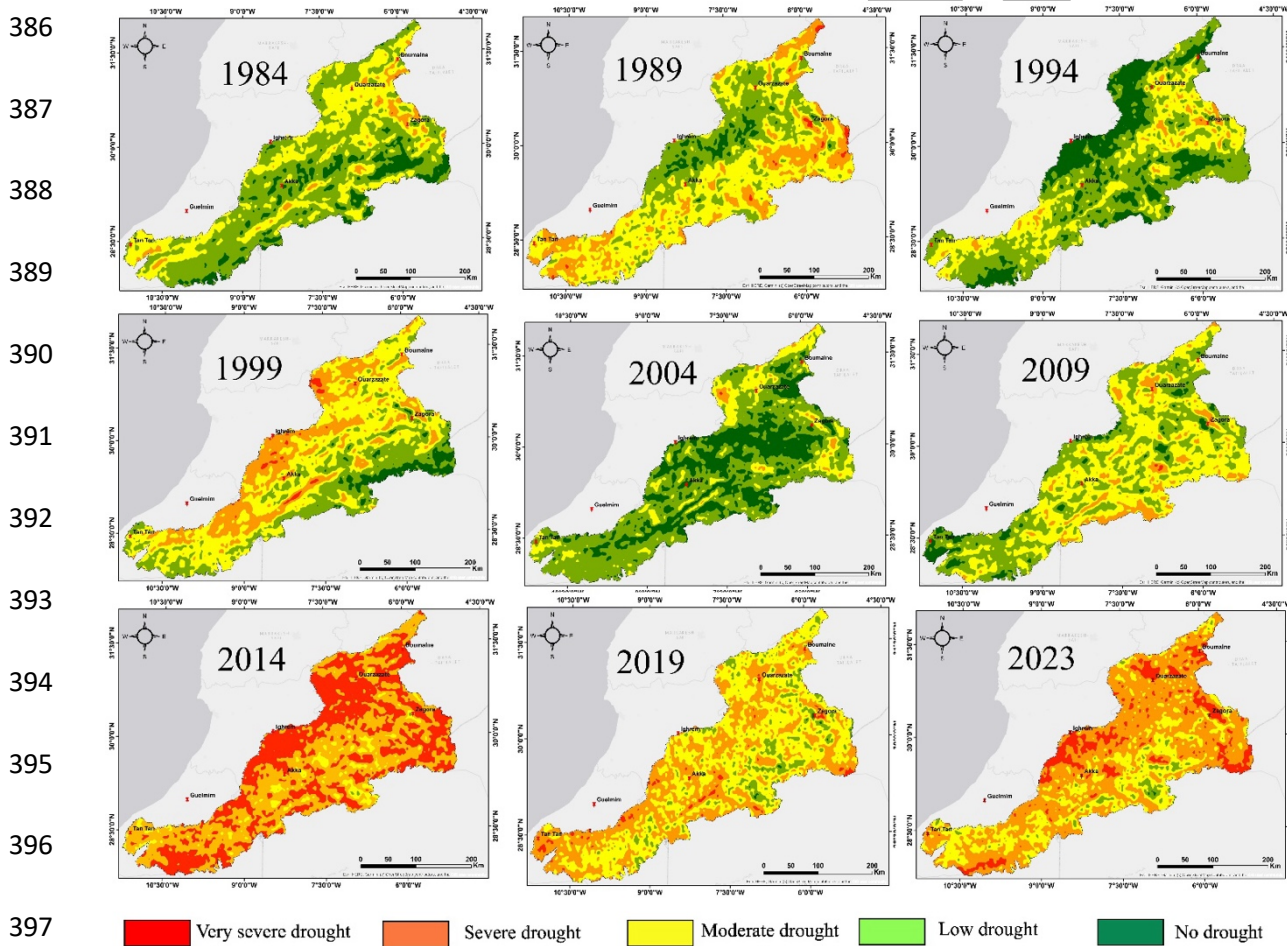


372 **Figure 5.** Spatiotemporal variation map of the Temperature Condition Index (TCI) illustrating
 373 thermal stress conditions across the study area during the observation period.

375 **Combined Reflectance and Brightness Temperature-Based Indices**

376 **VHI**

377 With regards to the Vegetation Health Index (VHI), the observed trends are consistent with
378 those of the NDVI, VCI and TCI. Initially, conditions appear favorable throughout the
379 watershed, with varying intensity due to the different microclimates of each region, influenced
380 by their specific topographic context. However, from 2004 onwards, the calculations show a
381 significant upheaval, with the class indicating unfavorable vegetation conditions invading
382 almost the entire watershed. This trend indicates an alarming drought, which can be
383 corroborated by the other indices based on the local meteorological conditions, hence the
384 importance of a multidimensional analysis of the indices for a complete and accurate
385 understanding of the drought in the study area.



398 **Figure 6.** Vegetation Health Index (VHI) variation map showing spatiotemporal changes in
399 vegetation health across the study area.

401 **Rainfall variation-based indices**

402 **SPI**

403 Analysis of the graph showing variations in the Standardized Precipitation Index (SPI) for the
404 Drâa watershed from 1950 to 2023 reveals several important trends (Figure 7). During this
405 period, the SPI shows marked variability, with prolonged episodes of severe drought,
406 particularly notable in the years 1961, 1962, 1976, 1982-1985, 1999-2002 and 2016-2023 (with
407 the exception of the year 2018-2019), when SPI values fall below -1.5, indicating exceptionally
408 dry conditions. In contrast, significant peaks of excess precipitation occur between 1952-1957,
409 1963-1969, 1988-1994, 1996-1998, 2003-2007, and 2014-2015, with SPI values reaching +1.5,
410 indicating periods of abundant precipitation.

411 The overall trend in the SPI appears to oscillate between periods of intense drought and excess
412 precipitation, with a notable variation in the frequency of events between the 1990s and 2000s.
413 Prior to 2002, droughts had a significant amplitude but a limited duration of 3 or 4 years at
414 most, while wet periods were more prolonged, with somewhat lower amplitudes. Since 2002,
415 wet periods have become rarer, with an average amplitude and generally lasting only one or
416 two consecutive years. On the other hand, a precipitation deficit extends over about 17 years,
417 from 2007 to 2023, with a few one-year breaks, as in 2014-2015 and 2018-2019. In terms of
418 SPI, over a period of 23 years (2000-2023) the watershed has experienced only 9 relatively wet
419 years compared with 14 dry years. These rainfall deficits, spread over a long period, and in
420 parallel with the rise in temperatures, confirms the results of the other indices reflecting
421 vegetation health.

422 **PDSI**

423 Variations in the Palmer Drought Severity Index (PDSI) corroborate the fluctuations observed
424 through the SPI indices (Figure 8). This is to be expected, as the Palmer index is based on
425 similar parameters to those used to assess rainfall deficits and surpluses. The periods most
426 severely affected by drought, identified by the lowest PDSI values, include the intervals 1982-
427 1984, 1999-2000, and the long dry period from 2015 to the present day. Conversely, wet periods
428 are less frequent, with significant peaks recorded in the years 1987-1989, 2002, and 2014. These
429 observations confirm the harmonization of drought and precipitation indices in the assessment
430 of climatic conditions in the watershed, underlining their complementarity in the analysis of
431 climatic trends.

432

433

434

435

436

437

438

439

440

441

442

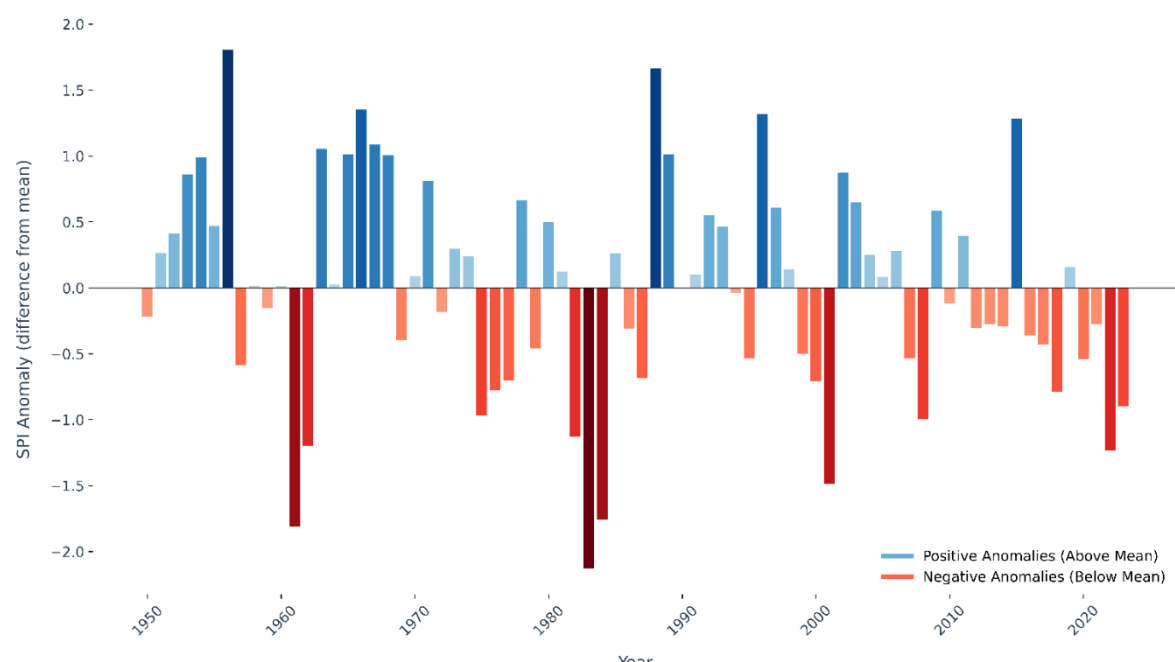
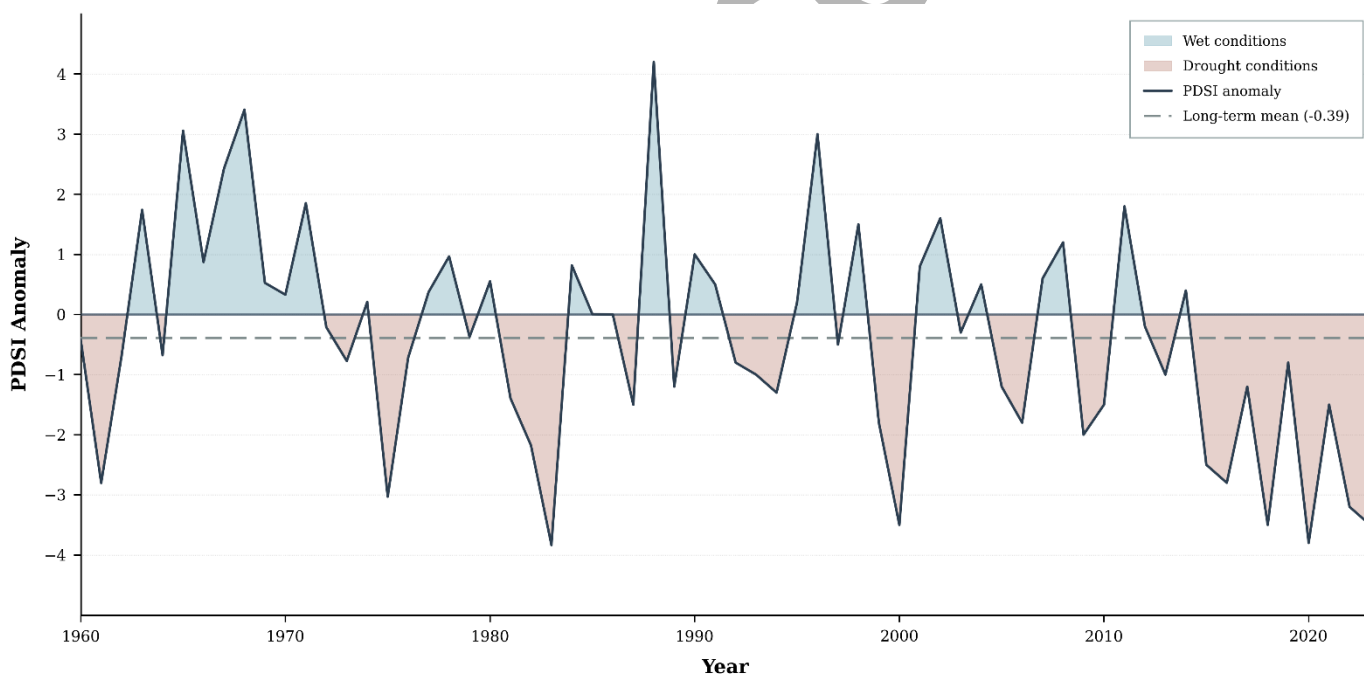


Figure 7. Variations of the Standardized Precipitation Index (SPI) illustrating the temporal evolution of meteorological drought conditions in the study area.



443

444

445

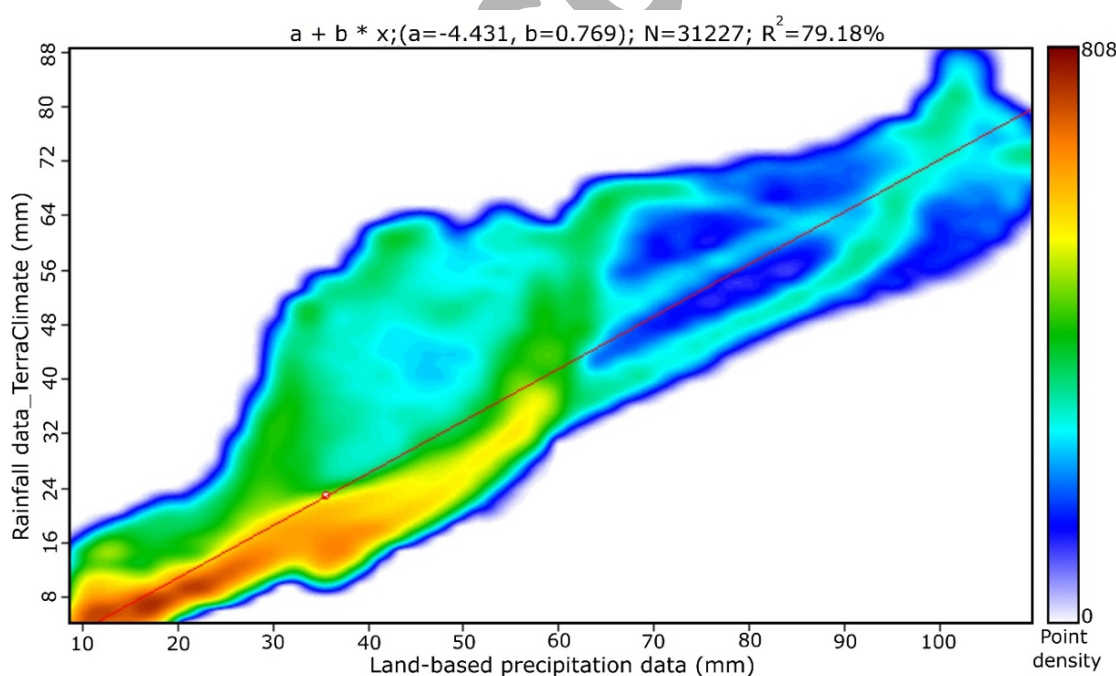
446

447 **Validation of findings**

448 **Observed climatic and hydrological parameters**

449 As a performance test, we implemented a rigorous validation, comparing the results with variations in
450 climatic parameters. Specifically, we compared precipitation data from 27 hydrological stations along
451 the Drâa River with temperatures provided by the TerraClimate satellite and with the results of drought
452 indices derived from remote sensing.

453 To assess the performance of the TerraClimate satellite itself, we compared spline-with-barriers
454 interpolation based on precipitation data provided by the Drâa-Oued Noun Hydraulic Basin Agency
455 with those derived from satellite observations. This comparison allowed us to calculate a correlation
456 index, which serves as a basis for assessing the accuracy of the data provided by TerraClimate. A high
457 correlation index, on the order of 79% (Figure 9), confirms the reliability of the satellite data. This not
458 only ensures the accuracy of the climate data used in our analyses, but also increases confidence in the
459 results obtained and their relevance to the assessment drought conditions and climate trends in the
460 Drâa catchment.

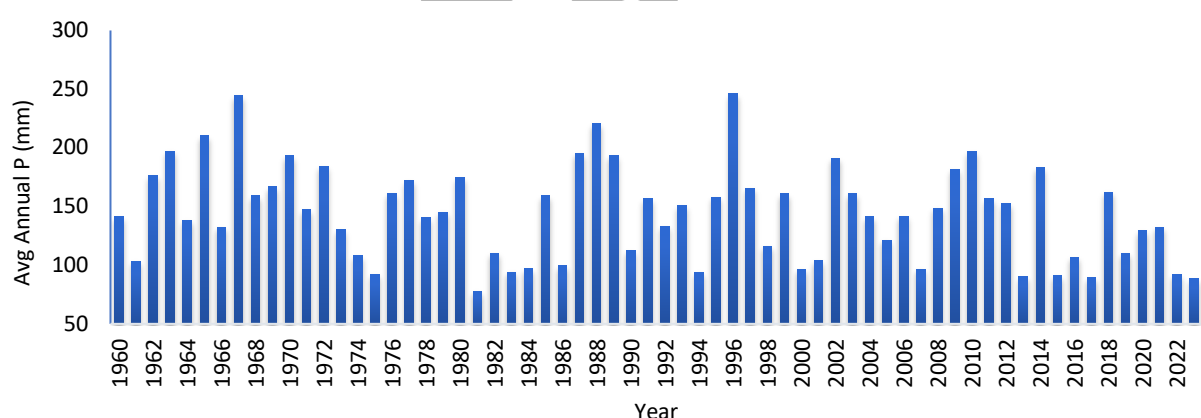


470 **Figure 9.** Results of the correlation analysis between TerraClimate precipitation data and ground-
471 based (in-situ) precipitation observations.

472 Figure 10 illustrates the variations in mean annual precipitation in the Drâa watershed, as determined
473 by “spline with barriers” interpolation using ArcGIS software, between 1960 and 2023. In general, the

474 pattern of oscillations reveals a downward trend in annual precipitation in the watershed over time.
475 There were significant precipitation peaks, with values reaching 244.5 mm in 1967, and 246.5 mm in
476 1996. In contrast, troughs reflect periods of low precipitation, with minimum values dropping to 85.9
477 mm in 2023. It is important to note that it has now been 27 years (1996-2023) since the Drâa watershed
478 recorded an average annual rainfall of more than 200 mm. This observation underscores a prolonged
479 downward trend in precipitation levels in the region, reflecting a significant change from previous
480 periods when higher values were common.

481 With regard to maximum temperatures (Figure 11), an interpolation based on satellite data provided
482 by TerraClimate shows variations in maximum temperatures in the Drâa watershed from 1960 to 2023.
483 The graph derived from this analysis shows a general trend of increasing temperatures over the past
484 several decades. Maximum temperatures have ranged from a low of 25.5°C in 1971 to a high of 30.6°C
485 in 2023. In other words, the region has experienced an average increase of 5°C over the past 52 years.
486 More specifically, in the last two decades, i.e. between 2000 and 2023, the maximum temperature has
487 risen by 3°C, from 27.6°C in 2000 to the peak recorded in 2023. This increasing trend in maximum
488 temperature raises significant concerns about the future impacts of global warming on the watershed.
489 It is crucial to consider how these changes could affect local ecosystems, water resources and living
490 conditions in the region as temperatures continue to rise.



491
492 **Figure 10.** Temporal variation in average annual precipitation in the Drâa Watershed, based on data
493 from ABHDON (2023).



494

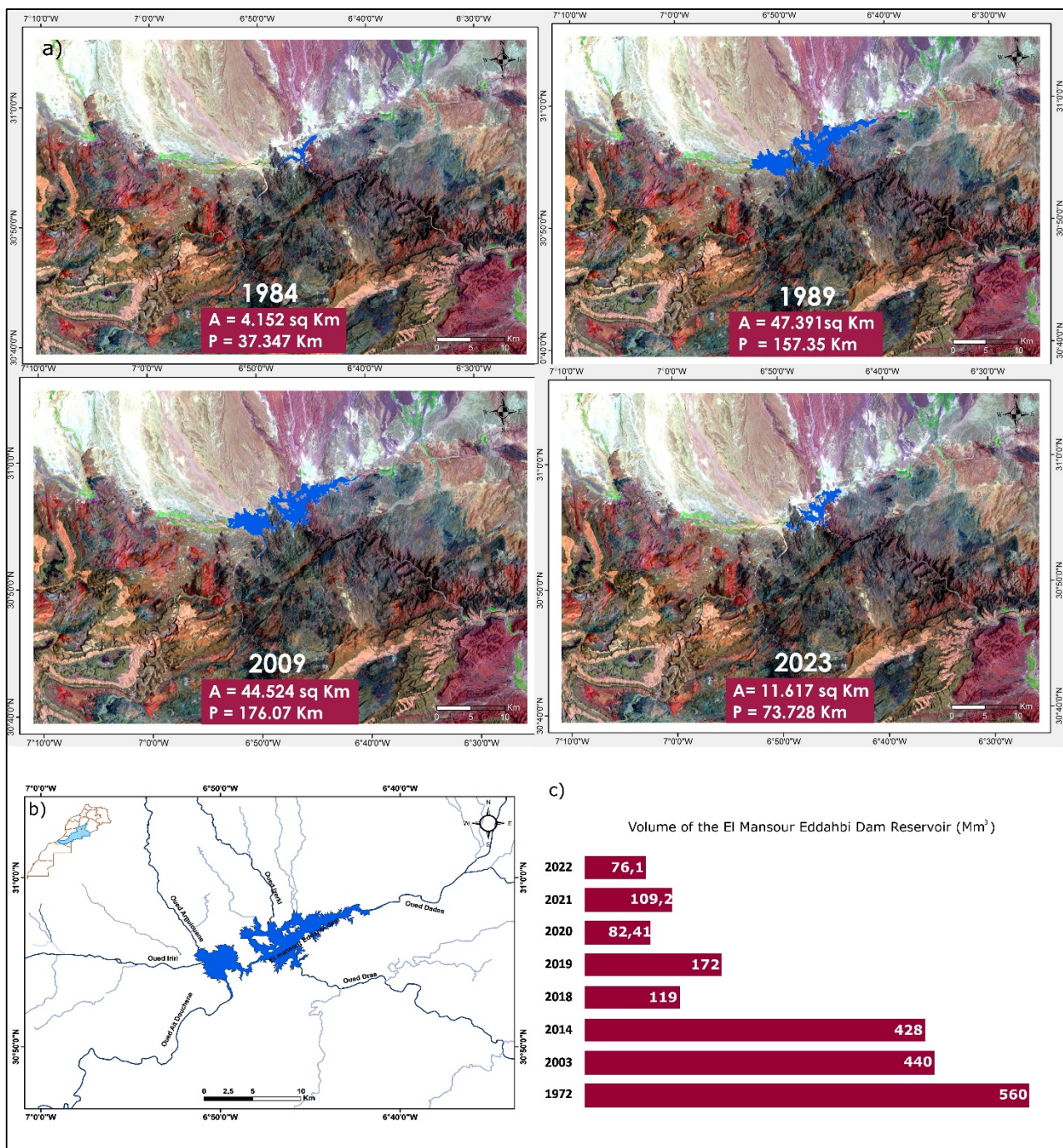
495 **Figure 11.** Temporal variation in the annual mean maximum temperatures in the Drâa Watershed,
 496 based on TerraClimate data (2023).

497 In a third validation step, we applied the Normalized Difference Water Index (NDWI) to the El
 498 Mansour Eddahbi reservoir to monitor its spatio-temporal evolution in response to climatic variations
 499 (Figure 12). Analysis of the data covering forty years, from 1984 to 2023, reveals the significant
 500 influence of rainfall deficits on the reservoir extent. In 1984, following two consecutive years of
 501 drought, a sharp reduction in the reservoir's water surface area was observed ($4,152 \text{ km}^2$). By contrast,
 502 in 1989, the wettest year of the period according to annual precipitation records, drought indices and
 503 vegetation vitality indices saw a substantial increase in reservoir surface area and perimeter (47.39 km^2
 504 and 157.35 km , respectively). Although wet years became less frequent after 2000, some, such as 2009,
 505 still resulted in significant increases in reservoir surface area and perimeter (44.52 km^2 and 176.07 km ,
 506 respectively). From that date onwards, the gradual decline in precipitation, combined with rising
 507 temperatures and increased evaporation rates, has severely affected water levels. By 2023, the reservoir
 508 had shrunk considerably (11 km^2 in area and 73 km in perimeter), clearly illustrating the devastating
 509 effects of drought on the regional water resources. Surface and perimeter variations derived from the
 510 NDWI were validated by reservoir volume measurements provided by the Drâa Oued Noun Water
 511 Agency, covering the period from dam construction in 1972 to 2023, with a particular focus on key
 512 years (Figure 12).

513

514

515



516 **Figure 12.** Variation in the water surface area and perimeter of the El Mansour Eddahbi Dam Reservoir
517 between 1984 and 2023 (a); location of the dam in relation to the tributaries of the Upper Drâa (b);
518 variation in the reservoir volume between 1972 and 2022 (c) (ABHDON, 2022)

519 **Discussions**

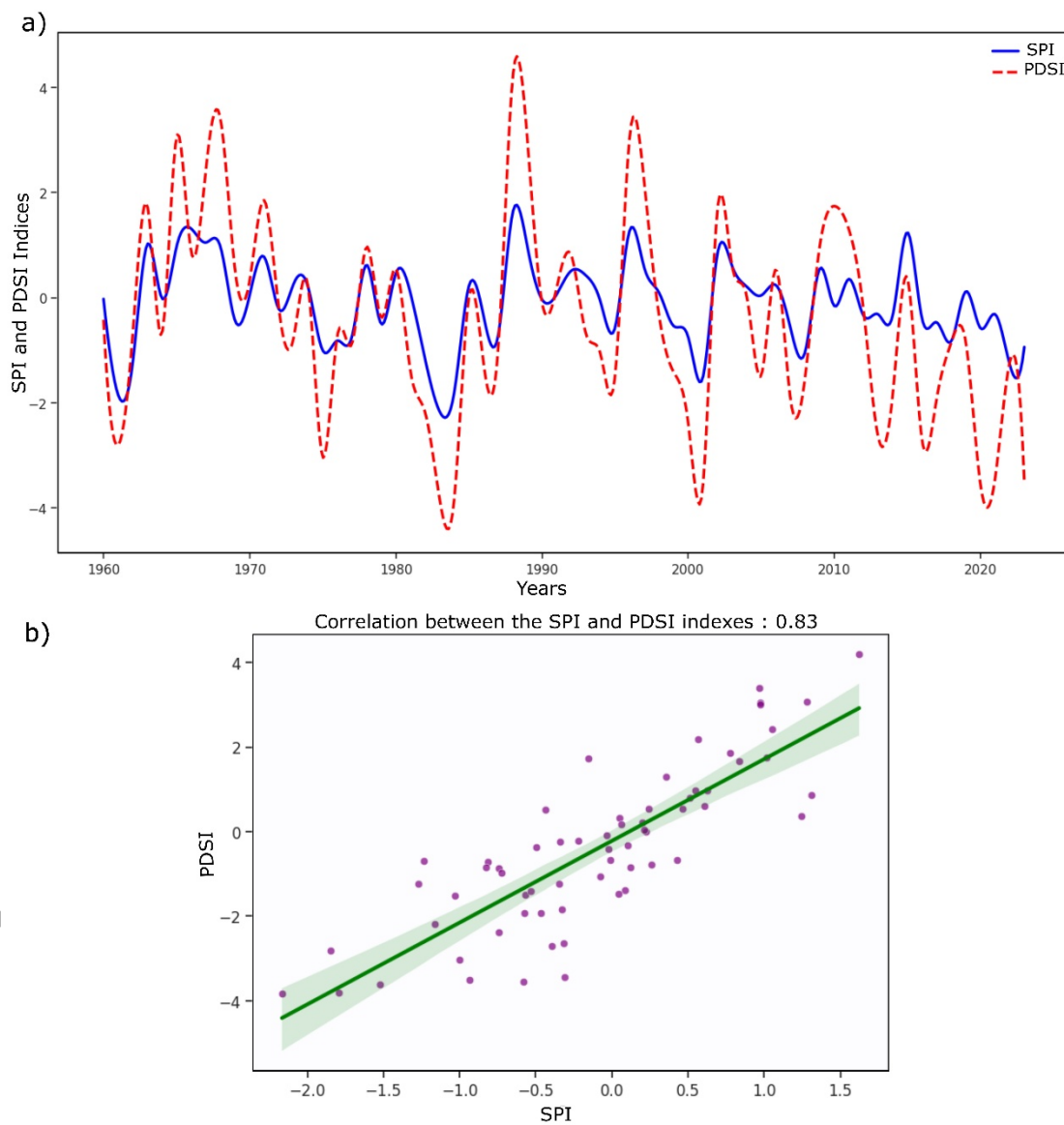
520 Vegetation indices include NDVI and NOAA indices include VCI, TCI and VHI. Although they are
521 based on different measurement principles - NDVI is based on the reflectance of vegetation surfaces,
522 while NOAA indices are based on brightness temperature - these indices ultimately show variations in

523 time and space, with a trend towards a decrease in vegetation cover in recent decades. It is important
524 not to interpret the results of these indices in isolation, as they provide only a partial overview of
525 vegetation health. Vegetation health can be adversely affected not only by periods of drought, but also
526 by flooding. In addition, heavy rainfall combined with extremely low temperatures can also adversely
527 affect vegetation health. It is therefore important to complement the analysis of these indices with other
528 information to obtain a complete picture. It should also be emphasized that the indices analyzed refer
529 to vegetation health for only the month of April over the nine years of comparison (1984, 1989, 1994,
530 1999, 2000, 2004, 2009, 2014, 2019, 2023). April is chosen as the reference month because at this time
531 vegetation growth is most sensitive to environmental conditions. This explains, for example, why the
532 drought indices show a severity in 2014, even though there was significant precipitation in that year
533 (Figures 10). Indeed, this precipitation only occurred in September, November and December, and not
534 during critical vegetation months such as April. Focusing on the variation in VHI index, an index that
535 assesses vegetation health by integrating vegetation conditions, we can observe that the health of the
536 vegetation cover varies according to topography, proximity to the High Atlas, and fluctuations in
537 meteorological parameters. One year is not enough to restore vegetation after three or four consecutive
538 years of drought, even if rainfall increases. In fact, vegetation health has deteriorated from 2009 to
539 2023, despite some slightly wetter periods between 2014-2015 and 2018-2020. The same trends apply
540 to the NDVI index, except that this index clearly illustrates the progression of desertification over most
541 of the watershed. The ubiquitous green belt (Figure 6) represents the south-facing slope of the High
542 Atlas, with their elevations and relatively favorable climate for crop development.

543 The results obtained from the SPI and PDSI indices show a strong correlation with variations in
544 precipitation and maximum temperatures. In fact, these indices confirm the trends revealed by the raw
545 climate data (Figures 10 and 11). To illustrate this correlation, it is relevant to look at the years
546 considered the wettest on the basis of high annual precipitation (244.5 mm in 1967, 222.6 mm in 1988
547 and 246.5 mm in 1996). In fact, the SPI indices for these years are 1.50 in 1967, 2.15 in 1988 and 1.80
548 in 1996. These high values indicate a period of exceptionally above-average rainfall, confirming the
549 trend towards wetter conditions during these years.

550 The PDSI is also part of this correlation with variations in raw climatic parameters. To illustrate this
551 correlation, we have analyzed in detail the years most prone to drought, as well as the wettest periods
552 according to the available data. The year 2023, for example, characterized by particularly dry
553 conditions, shows an extremely low PDSI index of -3.50, accompanied by a high average maximum
554 temperature of 30.6°C. This result confirms a severe and persistent drought situation. On the other
555 hand, the year 1971, which records the lowest mean maximum temperature (25.5°C) of the period

556 (1960-2023) and an annual rainfall of 147.8 mm, is associated with a PDSI index of 3.40. This value
 557 indicates relatively wet and humid conditions and suggests a low vulnerability to drought this year.
 558 The 83% positive correlation between the SPI and PDSI indices (Figure 13), illustrated by the
 559 scatterplot and fitted regression line, confirms their strong relationship, indicating that water deficits
 560 detected by the SPI are well reflected by the PDSI. PDSI increases when SPI increases, as precipitation
 561 is the main variable influencing both indices.



577 **Figure 13.** Comparison of the temporal evolution of the Standardized Precipitation Index (SPI) and
 578 the Palmer Drought Severity Index (PDSI) from 1960 to 2023 (a), and scatter plot showing the
 579 correlation between the SPI and the PDSI values (b).

580 The SPI measures precipitation anomalies directly, so when it is positive, it means that there is an
581 excess of rainfall compared to normal. Since the PDSI also incorporates this precipitation into its
582 calculation, an increase in the SPI generally indicates a recharge of soil moisture, thus reducing water
583 stress and leading to a rise in the PDSI. However, the PDSI responds more slowly to variations in SPI,
584 as it takes into account evapotranspiration and the soil's capacity to retain water, which can dampen or
585 delay its variations compared to the SPI.

586 The response of surface water bodies to weather conditions is often direct and rapid, particularly in
587 semi-arid environments where water availability is heavily influenced by rainfall variability and
588 evaporation processes. In this context, large reservoirs are highly sensitive indicators of hydroclimatic
589 stress. The El Mansour Eddahbi reservoir, which regulates surface water resources in the Upper Drâa
590 sub-basin, is an essential indicator for assessing the hydrological impacts of drought at the basin scale.
591 The results highlight a close link between climate variability and surface water dynamics, as evidenced
592 by the strong correlation between surface variations derived from NDWI and measured reservoir
593 volumes. Periods characterized by pronounced rainfall deficits lead to a rapid contraction in reservoir
594 extent, reflecting reduced inflows and increased evaporation due to rising temperatures. Conversely,
595 episodic wet years lead to short-lived recoveries in reservoir surface area, illustrating the system's
596 dependence on interannual precipitation variability rather than long-term storage resilience. Overall,
597 the consistency between the NDWI maps and the observed variations in reservoir volume confirms the
598 relevance of remote sensing-based hydrological indices for monitoring surface water dynamics in
599 regions where data are scarce.

600 Beyond validation objectives, these results highlight the vulnerability of surface water resources in the
601 Drâa basin to prolonged drought conditions and reinforce the importance of further studies in this
602 region for effective water resource management.

603 Conclusion

604 As part of this study, the results derived from satellite imagery were validated using ground-based data.
605 Today, data availability is no longer a major barrier to studying drought risk over time and space.
606 Thanks to sources such as NOAA and TerraClimate, along with band analysis from satellite images
607 like Landsat, Modis, and others, it is now possible to access essential global parameters. These datasets
608 allow for the calculation of various drought indices, enable correlation with observed conditions, and
609 support the development of representative maps illustrating the evolution of climatic situations. The
610 Drâa watershed, like much of Morocco, has long experienced alternating dry and wet periods.
611 However, in recent decades, the frequency of drought years has significantly increased, marked by

612 greater severity and broader spatial extent. The few relatively wet years are no longer sufficient to
613 restore water resources or regenerate vegetation cover. Located in the southern part of Morocco, the
614 Drâa Basin's climatic context makes it particularly vulnerable to meteorological, hydrological, and
615 hydrogeological droughts. Since the droughts of the 1980s, the region has shown a cyclic pattern of
616 alternating dry and wet seasons, with a recurrence interval of approximately two to three years. Yet,
617 since the 2000s, both the frequency and impact of drought years have intensified, particularly in terms
618 of vegetation loss and declining water availability in the reservoir of the El Mansour Eddahbi dam.
619 This situation is reflected in the variation of several indicators including the Vegetation Condition
620 Index (VCI), Temperature Condition Index (TCI), Vegetation Health Index (VHI), and the Normalized
621 Difference Vegetation Index (NDVI), along with climate-based indices including the Standardized
622 Precipitation Index (SPI), the Palmer Drought Severity Index (PDSI), and the Normalized Difference
623 Water Index (NDWI) applied to the dam reservoir. The interpretation of resulting maps and graphs
624 required an integrated approach, combining advanced remote sensing data with ground observations
625 from hydrological stations across the Drâa watershed, to ensure a coherent and comprehensive
626 analysis. Ultimately, the findings have confirmed that the observed variations closely follow the
627 fluctuations of key climatic parameters—namely, annual average precipitation and average maximum
628 temperatures.

629 **Acknowledgments**

630 We gratefully acknowledge the invaluable support of all individuals and institutions that contributed
631 to the completion of this study. Particular appreciation is extended to the Centre National pour la
632 Recherche Scientifique et Technique (CNRST), Rabat, Morocco, for its financial support through the
633 "PhD-Associate Scholarship" program. We also wish to thank the Agence du Bassin Hydraulique Drâa-
634 Oued Noun, with special recognition to its Director, Mr. Essanhajy, and hydrogeological engineer, Mr.
635 Aoujil, for their technical assistance and collaboration. We are especially grateful to the Ministère des
636 Relations internationales et de la Francophonie and the Natural Sciences and Engineering Research
637 Council of Canada for their support to the third and fourth authors, respectively.

638

639

640

641

Abatzoglou JT, 2013. Development of gridded surface meteorological data for ecological applications and modelling. *International Journal of Climatology*, 33(1) : 121–131. <https://doi.org/10.1002/joc.3413>

Agence du Bassin Hydraulique de Drâa Oued Noun (ABHDON), 2009. *Eaux de surface*. Avenue Mohamed VI, BP 1351, Guelmim, Maroc.

Agence du Bassin Hydraulique de Drâa Oued Noun (ABHDON), 2013. *Eaux de surface*. Avenue Mohamed VI, BP 1351, Guelmim, Maroc.

AghaKouchak A, Cheng L, Mazdiyasni O, Farahmand A, 2014. Global warming and changes in risk of concurrent climate extremes: Insights from the 2014 California drought. *Geophysical Research Letters*, 41(23) : 8847–8852. <https://doi.org/10.1002/2014GL062308>

Agoussine M, Bouchaou L, 2004. Les problèmes majeurs de la gestion de l'eau au Maroc. *Sécheresse*, 15(2) : 187–194.

Agoussine M, 2003. Les divers aspects de l'hydrologie en régions arides et semi-arides – cas du sud-est marocain. *Terre & Vie*, Rabat, 70.

Agoussine M, Saidi MEM, Igoumoullan B, 2004. Reconnaissance des ressources en eau du bassin d'Ouarzazate (Sud-Est marocain). *Bulletin de l'Institut Scientifique, Rabat, section Sciences de la Terre*, 26 : 81–92.

Aït Hamza M, El Faskaoui B, Fermin A, 2010. Les oasis du Drâa au Maroc. *Hommes & Migrations*, 1284 : 56–69.

Ait Dhmane L, Saidi ME, Moustadraf J, Rafik A, Hadri A, 2024. Spatiotemporal characterization and hydrological impact of drought patterns in northwestern Morocco. *Frontiers in Water*, 6 : 1463748. <https://doi.org/10.3389/frwa.2024.1463748>

Aksu H, Cetin M, Aksoy H, Yaldiz SG, Yildirim I, Keklik G, 2022. Spatial and temporal characterization of standard duration-maximum precipitation over Black Sea Region in Turkey. *Natural Hazards*, 111(3) : 2379–2405. <https://doi.org/10.1007/s11069-021-05141-6>

Alley WM, 1984. The Palmer Drought Severity Index: Limitations and assumptions. *Journal of Applied Meteorology and Climatology*, 23(7) : 1100–1109. [https://doi.org/10.1175/1520-0450\(1984\)023<1100:TPDSIL>2.0.CO;2](https://doi.org/10.1175/1520-0450(1984)023<1100:TPDSIL>2.0.CO;2)

Auclair L, 1987. Maroc présaharien : bois de feu et désertification. *Forêt Méditerranéenne*, 9(1) : 41–48.

Bentaleb A, 2011. Pompage d'eau et désertification dans la Moyenne Vallée du Draâ : le cas du palmier Mezguita (Maroc). *Insaniyat*, 51–52. <https://doi.org/10.4000/insaniyat.1257>

Bentaleb A, 2015. Vulnérabilité oasienne : valorisation et développement territorial dans les zones arides marocaines. Cas : Oasis du Drâa moyen. Dans : *XIV^e Conférence Internationale Annuelle de l'Intelligence Territoriale “Développement durable des territoires vulnérables”*, octobre 2015, Ouarzazate, Maroc. <https://halshs.archives-ouvertes.fr/halshs-01741493>

Baki S, Hilali M, Kacimi I, Mahboub A, 2017. Caractérisation hydrogéologique et cartographie des ressources en eau dans le bassin versant de l'oued Rhéris (Sud-Est du Maroc). *Bulletin de l'Institut Scientifique, Rabat, Section Sciences de la Terre*, 38 : 29–43.

Bashit N, Ristianti N, Ulfiana D, 2022. Drought assessment using remote sensing and geographic information systems (GIS) techniques (Case study: Klaten District). *International Journal of Geoinformatics*, 18(5) : 115–127. <https://doi.org/10.52939/ijg.v18i5.2393>

Bijaber N, El Hadani D, Saidi M, Svoboda MD, Wardlow BD, Hain CR, Poulsen CC, Yessef M, Rochdi A, 2018. Developing a remotely sensed drought monitoring indicator for Morocco. *Geosciences*, 8(2) : 55. <https://doi.org/10.3390/geosciences8020055>

Bijaber N, Rochdi A, Yessef M, El Yacoubi H, 2024. Mapping the structural vulnerability to drought in Morocco. *International Journal of Engineering and Geosciences*, 9(2) : 264–280.

Briffa KR, Jones PD, Hulme M, 1994. Summer moisture variability across Europe, 1892–1991: An analysis based on the Palmer Drought Severity Index. *International Journal of Climatology*, 14(5) : 475–506. <https://doi.org/10.1002/joc.3370140502>

Cherkaoui Dekkaki H, 2001. Contribution à l'étude hydrogéologique des nappes alluviales de Fezouata et Ktaoua (Moyenne vallée du Drâa). Mémoire de D.E.S.A., École Mohammadia d'Ingénieurs, Rabat, Maroc.

Choukrani G, Hilali A, Bouri S, 2018. Diagnostic et projection future du changement climatique en zone aride : Cas de la région Marrakech-Safi (Maroc). *Larhyss Journal*, 36 : 49–63.

Cook ER, Meko DM, Stahle DW, Cleaveland MK, 1999. Drought reconstructions for the continental United States. *Journal of Climate*, 12(4) : 1145–1162. [https://doi.org/10.1175/1520-0442\(1999\)012](https://doi.org/10.1175/1520-0442(1999)012)

Dahan S, 2017. Gestion de la rareté de l'eau en milieu urbain au Maroc. *Banque mondiale*, Washington, DC. <https://documents1.worldbank.org/curated/en/48809151613312338/pdf/summary-report.pdf>

Direction de la Recherche et de la Planification de l'Eau (DRPE), 2008. Étude d'actualisation du plan directeur d'aménagement intégré des ressources en eau (PDAIRE) du bassin hydraulique du Drâa. Marché n°106/2008/DRPE, Rapport inédit.

Wilhite DA, Sivakumar MVK, Wood DA (éds), 2000. *Early Warning Systems for Drought Preparedness and Drought Management*. Actes de la réunion d'experts tenue à Lisbonne, Portugal, 5–7 septembre 2000. Genève, Suisse : Organisation météorologique mondiale.

El Qorchi F, Yacoubi Khebiza M, Omondi OA, Karmaoui A, Pham QB, Acharki S, 2023. Analyzing temporal patterns of temperature, precipitation, and drought incidents: A comprehensive study of environmental trends in the Upper Drâa Basin, Morocco. *Water*, 15(22) : 3906. <https://doi.org/10.3390/w15223906>

Elair C, Rkha Chaham K, Hadri A, 2023. Assessment of drought variability in the Marrakech-Safi region (Morocco) at different time scales using GIS and remote sensing. *Water Supply*, 23(11) : 4592–4624. <https://doi.org/10.2166/ws.2023.283>

Eyoh A, Okeke F, Ekpa A, 2019. Assessment of the effectiveness of the vegetation condition index (VCI) as an indicator for monitoring drought condition across the Niger Delta region of Nigeria using AVHRR/MODIS NDVI. *European Journal of Earth and Environment*, 6(1).

Gumus V, El Moçayd N, Seker M, Seaid M, 2024. Future projection of droughts in Morocco and potential impact on agriculture. *Journal of Environmental Management*, 367 : 122019. <https://doi.org/10.1016/j.jenvman.2024.122019>

Hadri A, Saidi MEM, El Khalki EM, Aachrine B, Saouabe T, Elmaki AA, 2022. Integrated water management under climate change through the application of the WEAP model in a Mediterranean arid region. *Journal of Water and Climate Change*, 13(6) : 2414–2442. <https://doi.org/10.2166/wcc.2022.039>

Hadria R, Boudhar A, Ouatiki H, Lebrini Y, Elmansouri L, Gadouali F, Hayat Lionboui HL, Benabdelouahab T, 2019. Combining use of TRMM and ground observations of annual precipitations for meteorological drought trends monitoring in Morocco. *American Journal of Remote Sensing*, 7(2) : 25. <https://doi.org/10.11648/j.ajrs.20190702.11>

Hao Z, Singh VP, 2015. Drought characterization from a multivariate perspective: A review. *Journal of Hydrology*, 527 : 668–678. <https://doi.org/10.1016/j.jhydrol.2015.05.031>

Houmma H, Ismaguil I, Gadal S, El Mansouri L, Garba M, Gbetkom PG, Mamane Barkawi MB, Hadria R, 2023. A new multivariate agricultural drought composite index based on random forest algorithm and remote sensing data developed for Sahelian agrosystems. *Geomatics, Natural Hazards and Risk*, 14(1) : 2223384. <https://doi.org/10.1080/19475705.2023.2223384>

Justice CO, Vermote E, Townshend JRG, Defries R, Roy DP, Hall DK, Salomonson VV, Privette JL, Riggs G, Strahler A, Lucht W, Myneni RP, Knyazikhin Y, Running SW, Nemani RR, Wan Z, Huete AR, van Leeuwen W, Wolfe RE, Giglio L, Muller J-P, Lewis P, Barnsley MJ, 1998. The Moderate Resolution Imaging Spectroradiometer (MODIS): Land remote sensing for global change research. *NASA Publications*, 28. <https://digitalcommons.unl.edu/nasapub/28>

Kim J-S, Park S-Y, Lee J-H, Chen J, Chen S, Kim T-W, 2021. Integrated drought monitoring and evaluation through multi-sensor satellite-based statistical simulation. *Remote Sensing*, 13(2) : 272. <https://doi.org/10.3390/rs13020272>

Kogan FN, 1990. Remote sensing of weather impacts on vegetation in non-homogeneous areas. *International Journal of Remote Sensing*, 11(8) : 1405–1419. <https://doi.org/10.1080/01431169008955102>

Kogan FN, 1997. Global drought watch from space. *Bulletin of the American Meteorological Society*, 78(4) : 621–636. [https://doi.org/10.1175/1520-0477\(1997\)078](https://doi.org/10.1175/1520-0477(1997)078)

Kogan FN, Sullivan J, 1993. Development of global drought-watch system using NOAA/AVHRR data. *Advances in Space Research*, 13(5) : 219–222. [https://doi.org/10.1016/0273-1177\(93\)90548-P](https://doi.org/10.1016/0273-1177(93)90548-P)

Lahbous M, Touzani L, Ousidahou A, 2023. La sécheresse et son impact sur l'économie marocaine. *La Revue d'économie et d'environnement*, 3(2) : 20–42. <https://revuecoenvi.org/index.php/laree/article/view/28>

Layelmam M, 2015. Calcul des indicateurs de sécheresse à partir des images NOAA/AVHRR. Rapport de recherche, IAV, CRTS, CRASTE-LF. <https://hal.archives-ouvertes.fr/hal-00915461>

Lebdi F, Maki A, 2023. La sécheresse au Maghreb : diagnostic, impacts et perspectives pour le renforcement de la résilience du secteur agricole. Tunis : FAO. <https://doi.org/10.4060/cc7126fr>

Ji L, Peters AJ, 2003. Assessing vegetation response to drought in the northern Great Plains using vegetation and drought indices. *Remote Sensing of Environment*, 87(1) : 85–98. [https://doi.org/10.1016/S0034-4257\(03\)00174-3](https://doi.org/10.1016/S0034-4257(03)00174-3)

Li J, Zhou S, Hu R, 2016. Hydrological drought class transition using SPI and SRI time series by loglinear regression. *Water Resources Management*, 30(2) : 669–684. <https://doi.org/10.1007/s11269-015-1184-7>

Liu W, Kogan FN, 2002. Monitoring Brazilian soybean production using NOAA/AVHRR based vegetation condition indices. *International Journal of Remote Sensing*, 23 : 1161–1179.

McFeeters SK, 1996. The use of the normalized difference water index (NDWI) in the delineation of open water features. *International Journal of Remote Sensing*, 17(7) : 1425–1432. <https://doi.org/10.1080/01431169608948714>

McKee TB, Doesken NJ, Kleist J, 1993. The relationship of drought frequency and duration to time scales. Dans : *Proceedings of the 8th Conference on Applied Climatology*, 179–186. American Meteorological Society.

McKee TB, Doesken NJ, Kleist J, 1995. Drought monitoring with multiple time scales. Dans : *Proceedings of the 9th Conference on Applied Climatology*, 233–236. American Meteorological Society, Dallas, TX.

Mehdaoui R, Mili EM, Seghir A, 2018. Caractérisation à l'aide du SPI de la sécheresse climatique dans le bassin versant de Ziz (Sud-Est, Maroc). *European Scientific Journal*, 14(21) : 177–194.

Ouysse S, Laftouhi N-E, Tajeddine K, 2010. Impact of climate variations on water resources in the Drâa basin (Morocco): Correlation between precipitation and evapotranspiration variability in the Drâa basin. Dans : *Proceedings of the International Conference on Participatory and Integrated Management of Water Resources in Arid Zones (GIRE3D)*, Ouarzazate, Morocco.

Palmer WC, 1965. Meteorological drought. Office of Climatology Research Paper No. 45. Washington DC : US Weather Bureau.

Rouse JW, Haas RH, Schell JA, Deering DW, 1973. Monitoring vegetation systems in the Great Plains with ERTS (Earth Resources Technology Satellite). Dans : *Proceedings of 3rd Earth Resources Technology Satellite Symposium*, Greenbelt, MD, USA, décembre 10–14, pp. 309–317.

Sadiki A, Hanchane M, 2024. Apport des SIG et de la télédétection dans le suivi et la cartographie du lac de barrage Mansour Eddahbi (Sud-Est du Maroc). *Espaces, Revue de Géographie*, (11-12) : 19–25.

Saouabe T, Naceur KA, El Khalki EM, Hadri A, Saidi ME, 2022. GPM-IMERG product: A new way to assess the climate change impact on water resources in a Moroccan semi-arid basin. *Journal of Water and Climate Change*, 13(7) : 2559–2576. <https://doi.org/10.2166/wcc.2022.403>

Schulz W, 2004. Reconstructing mediatization as an analytical concept. *European Journal of Communication*, 19(1) : 87–101. <https://doi.org/10.1177/0267323104040696>

Schulz O, Busche H, Benbouziane A, 2008. Decadal precipitation variances and reservoir inflow in the semi-arid Upper Drâa Basin (South-Eastern Morocco). Dans : Zereini F, Hötzl H (éds). *Climatic Changes and Water Resources in the Middle East and North Africa*, Environmental Science and Engineering, pp. 165–178. Springer, Berlin, Heidelberg. https://doi.org/10.1007/978-3-540-85047-2_13

Scian B, Donnari M, 1997. Retrospective analysis of the Palmer Drought Severity Index in the semi-arid Pampas region, Argentina. *International Journal of Climatology*, 17(3) : 313–322. [https://doi.org/10.1002/\(SICI\)1097-0088\(19970315\)17:3<313::AID-JOC112>3.0.CO;2-W](https://doi.org/10.1002/(SICI)1097-0088(19970315)17:3<313::AID-JOC112>3.0.CO;2-W)

Seiler RA, Kogan F, Sullivan J, 1998. AVHRR-based vegetation and temperature condition indices for drought detection in Argentina. *Advances in Space Research*, 21(3) : 481–484. [https://doi.org/10.1016/S0273-1177\(97\)00884-3](https://doi.org/10.1016/S0273-1177(97)00884-3)

Serbouti I, Chenal J, Pradhan B, Diop EB, Azmi R, Abdem SAE, Adraoui M, Hlal M, Bounabi M, 2024. Assessing the impact of agricultural practices and urban expansion on drought dynamics using a multi-drought index application implemented in Google Earth Engine: A case study of the Oum-Er-Rbia watershed, Morocco. *Remote Sensing*, 16 : 3398. <https://doi.org/10.3390/rs16183398>

Stour L, Agoumi A, 2008. Climatic drought in Morocco during the last decades. *Hydroéologie Appliquée*, 16 : 215–232.

Wang Q, Shi P, Lei T, Geng G, Liu J, Mo X, Li X, Zhou H, Wu J, 2015. The alleviating trend of drought in the Huang-Huai-Hai Plain of China based on the daily SPEI. *International Journal of Climatology*, 35(13) : 3760–3769. <https://doi.org/10.1002/joc.4244>

Waroux YLP, 2013. Dégradation environnementale et développement économique dans l’arganeraie d’Aoulouz (Maroc). *Sécheresse*, 24(1) : 29–38.

Weber B, 2004. Untersuchungen zum Bodenwasserhaushalt und Modellierung der Bodenwasserflüsse entlang eines Höhen- und Ariditätsgradienten (SE Marokko). Thèse de doctorat.

Wilhite DA, 2000. Drought planning and risk assessment: status and future directions. *Annals of Arid Zone*, 39 : 211–230.

World Meteorological Organization (WMO), 2012. Standardized precipitation index user guide (M. Svoboda, M. Hayes, & D. Wood). WMO-No. 1090. Genève : WMO. https://library.wmo.int/viewer/31481/download?file=wmo_1090_fr.pdf&navigator=1&type=pdf

Zhang A, Jia G, 2013. Monitoring meteorological drought in semiarid regions using multi-sensor microwave remote sensing data. *Remote Sensing of Environment*, 134 : 12–23. <https://doi.org/10.1016/j.rse.2013.02.023>

Zkhiri W, Tramblay Y, Hanich L, Jarlan L, Ruelland D, 2018. Spatiotemporal characterization of current and future droughts in the High Atlas basins (Morocco). *Theoretical and Applied Climatology*, 135(1-2) : 593–605. <https://doi.org/10.1007/s00704-018-2388-6>